Int. J. Electrochem. Sci., 13 **(2018)** 3420 – 3428, doi: 10.20964/2018.04.48

International Journal of
ELECTROCHEMICAL
SCIENCE
www.electrochemsci.org

Development of a Metal-Organic Framework for the Sensitive Determination of 2,4-Dichlorophenol

Meng Cui[1,2], *Jingtong Li*[2], *Dayong Lu*[2,*], *Ziqiang Shao*[1,*]

[1] Beijing Engineering Research Center of Cellulose and Its Derivatives, School of Materials Science and Engineering, Beijing Institute of Technology, Beijing, 100081, P.R. China
[2] College of Materials Science and Engineering, Jilin Institute of Chemical Technology Research Center for Materials Science and Engineering, Jijin, 132022, P.R. China
[*]E-mail: cm860502@163.com

Received: 10 December 2017 / *Accepted:* 30 January 2018 / *Published:* 6 March 2018

The present study proposed a facile and highly sensitive electrochemical sensor based on a carbon paste electrode modified by the metal–organic framework (MOF) [Cu(bpy)(H_2O)$_2$(BF_4)$_2$(bpy)] for the analysis of 2,4-dichlorophenol (2,4-DCP). X-ray diffraction (XRD) and Fourier transform infrared spectrometry (FT-IR) were used to investigate the morphology and composition, respectively, of [Cu(bpy)(H_2O)$_2$(BF_4)$_2$(bpy)]. Additionally, cyclic voltammetry (CV) was carried out to study the electrochemical performance. Considering the high charge transfer efficiency, strong adsorption capacity and large specific surface area of [Cu(bpy)(H_2O)$_2$(BF4)$_2$(bpy)], our developed sensor was favorably selective to the detection of 2,4-DCP under optimum parameters, with a wide linear range of 4 to 100 μM and a low limit of detection (LOD) of 1.1 μM.

Keywords: Metal–organic frameworks; [Cu(bpy)(H_2O)$_2$(BF_4)$_2$(bpy)]; 2,4-dichlorophenol; Electrochemical determination; Sensor

1. INTRODUCTION

Chlorophenol, an environmental pollutant, has recently attracted considerable attention. Chlorophenols have a direct and an indirect impact on both the animal populations and aquatic ecosystems, and thus have been widely used as intermediates in dyes, biocides and leather and wood preservation as well as in chemical raw materials [1-3]. The transportation of chlorophenol in sediment, water and soil depends on the chlorine atom number and pH of the environment. These semivolatile organochlorine compounds are persistent in receiving aquatic environments and could be detected in natural surroundings, including bottom sediments, surface and ground waters [4-7]. Among the priority pollutants, 2,4-dichlorophenol (2,4-DCP) occupies a vital position, according to the United

States Environmental Protection Agency (US EPA) [8, 9]. Additionally, 2,4-DCP has been presumed to be an endocrine disruptor in recent years [10-13].

2,4-DCP irritates the respiratory tract after the inhalation and is detrimental to the liver, kidneys, and blood-forming organs [14-17]. Additionally, some of the humans and animals exposed to 2,4-DCP have shown serious injury to the upper respiratory tract and permanent vision impairment or even blindness [18-21], which demonstrates a certain degree of toxicity. Therefore, it is urgent to develop accurate, sensitive, rapid, and facile analytical strategies to detect and quantify this compound. To date, a few related approaches have been reported, including the use of gas chromatography [22-24], liquid chromatography [25, 26], UV-spectrophotometry [27] and chemiluminescence [28, 29] methods. The above strategies utilize inconvenient and complex sample preparation procedures for the *in situ* experiments, despite wide working concentration ranges and low limits of detection (LODs) [30]. In contrast, electrochemical sensors could provide an on-the-spot analysis of real samples, due to their distinct response speed, low cost of preparation, facile instrumentation, and high sensitivity [31, 32].

As prominent crystalline inorganic–organic hybrid materials, MOFs have three-dimensional ordered frameworks, where organic ligands and metal clusters are connected in space [33-36]. MOFs have high chemical stability, large surface areas, and high pore volumes and thus are considered intriguing materials [37, 38] that can be used in many different fields, such as sensing, drug delivery, catalysis, separation, and gas storage [39, 40]. Hosseini and co-workers [41] proposed the use of Au–SH–SiO_2 nanoparticles supported on the metal-organic framework Au–SH–SiO_2@Cu-MOF for the fabrication of an electrochemical sensor for the analysis of l-cysteine. Fu and co-workers [42] reported the development of a novel type of efficient MOF matrix for the immobilization of enzymes based on 2,5-dimercapto-1,3,4-thiadiazole, Na_2PtCl_6 and $NaAuCl_4$ for the amperometric biosensing of glucose or phenols. $Cu_3(BTC)_2$, a characteristic MOF material, is highly conductive with a loose, porous and snowflake-like structure, which has been acknowledged as an excellent material for electrochemical analysis. However, the application of the MOF-modified electrochemical sensors for the detection of 2,4-DCP has not been reported.

The present study reported the synthesis of the MOF [Cu(bpy)$(H_2O)_2(BF4)_2$(bpy)] along with its characterization using X-ray diffraction (XRD) and Fourier transform infrared spectrometry (FT-IR). In addition, [Cu(bpy)$(H_2O)_2(BF4)_2$(bpy)] was used for the preparation of a highly sensitive electrochemical sensor for 2,4-DCP analysis, and a reaction mechanism associated with 2,4-DCP oxidization was reported.

2. EXPERIMENTS

2.1. Chemicals

Hydrated CuII tetrafluoroborate (Cu: 21–22 mass%), 4,4’-bipyridine and styrene oxide were purchased from Sinopharm Chemical Reagent Co., Ltd. Methanol, 2,4-DCP, isopropanol and tert-butanol were purchased from Aladdin. For the synthesis of the phosphate buffer solutions (PBS; 1 M;

pH: 4.0 - 9.0), standard stock solutions of KH_2PO_4 and K_2HPO_4 were mixed together while tuning the pH using NaOH (0.1 M) or H_3PO_4 (0.1 M).

2.2. [Cu(bpy)(H_2O)$_2$($BF4$)$_2$(bpy)] preparation

The preparation of [Cu(bpy)(H_2O)$_2$($BF4$)$_2$(bpy)] was conducted via deposition from aqueous ethanol based on a method reported elsewhere [43]. A mixture was obtained by dissolving 0.309 g $Cu(BF_4)2{\cdot}H_2O$ (1 mM) in 8 mL water. After the slow addition of a solution of 0.312 g 4,4'-bipyridine (2 mM) in 2 mL ethanol at ambient temperature, a blue precipitate was gradually yielded. These steps were followed by a stirring of the slurry at ambient temperature for 4 h. Then, the solid was filtered off, followed by washing using water and ethanol, drying at ambient temperature in air and at 100 °C under vacuum. The final product was stored under Ar before use.

2.3. Characterizations

Infrared spectra of the solid samples wetted with alcohol drops were plotted using a Bruker Vertex 70 spectrometer equipped with an attenuated total reflection infrared (ATR-IR) attachment (Harrick, MVP) and a liquid-nitrogen-cooled MCT detector at 1 cm^{-1} resolution. XRD measurements were carried out using a Siemens D5000 powder diffraction system with CuKα radiation (45 kV and 35 mA) and Cu as the reference to study the crystalline structure.

2.4. Electrochemical determination of 2,4-DCP

All electrochemical experiments were carried out using a CHI660D electrochemical workstation (Shanghai Chenhua Co. China) with a typical three-electrode assembly, where the working, reference, and auxiliary electrodes were a bare or a modified carbon paste electrode (CPE), a saturated calomel electrode (SCE), and a platinum wire, respectively. The test potentials were applied against the SCE. The preparation of the [Cu(bpy)(H_2O)$_2$($BF4$)$_2$(bpy)]-coated electrode followed the same procedure; only varying amounts of [Cu(bpy)(H_2O)$_2$($BF4$)$_2$(bpy)] were coated onto the CPE. Note that the electrode needed to be rinsed with double-distilled water and activated in a 0.1 M PBS (pH 7.0) solution by cyclic voltammetry (CV) until a stable blank background was obtained in the potential range from −0.1 to 1.0 V at a scan rate of 100 mV/s.

3. RESULTS AND DISCUSSION

As shown in the ATR-IR spectrum in Figure 1, several bands characteristic of structural water, bpy, and BF_4^- were observed for the [Cu(bpy)(H_2O)$_2$($BF4$)$_2$(bpy)] MOF. For the BF_4^- anion, intense and broad bands were found over a range of 950 to 1100 cm^{-1}. Under a free environment, the BF_4^- anion showed a symmetric stretching band; while in our case, it exhibited a very distorted asymmetric

stretching band, where a few prominent sharp bands can be observed [44, 45]. Therefore, it can be presumed that the BF_4^- anion in our case existed in a strongly asymmetric environment. At approximately 1612, 1411, 1223, and 824 cm^{-1}, doublet characteristics were shown for the bpy. The former two bands indicated ring stretching modes, whereas the other two bands corresponded to the in-plane and out-of-plane CH bending modes. On the other hand, the 1800–3700 cm^{-1} band was ascribed to structural H_2O in Cu-MOF, as shown in Figure 1. At 3492 cm^{-1}, a significant OH stretching band was found. Based on the comparison of the diffuse reflectance IR spectra between the Cu-MOF and dehydrated Cu-MOF, it can be presumed that the two bands at 1700–2000 cm^{-1} and 2000–3000 cm^{-1} corresponded to the hydrogen-bonding network.

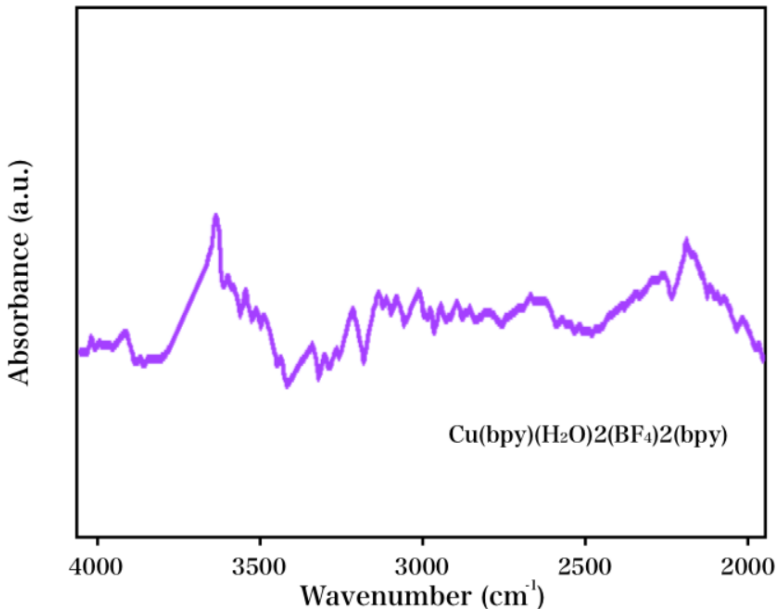

Figure 1. FTIR spectrum of $[Cu(bpy)(H_2O)_2(BF_4)_2(bpy)]$ recorded in powder form.

For the Cu-MOF, the high purity of the crystalline phases was confirmed by the XRD characterizations. As shown in Figure 2, typical peaks were observed at 6.87°, 9.64°, 11.83°, 13.42° and 19.31° at small 2θ angles, consistent with the results of a previous study results [46]. Significantly sharp XRD peaks were found, which suggested the high crystalline property of the as-prepared Cu-MOF. Additionally, the above peaks indicated that the Cu-MOF had a face-centered-cubic structure [47].

CV measurements were carried out for these electrodes in the presence of $K_3[Fe(CN)_6]$ (60 μM) in PBS (0.1 M, pH 7.2). Compared with the bare CPE, the CPE after modification with Cu-MOF showed a much larger peak current (I_p) (Figure 3). It was found that the difference between the peak potentials (ΔE_p) was reduced, which suggested that the Cu-MOF/CPE was more reversible. Obviously, the composite electrode became more conductive after the functionalization with Cu-MOF and an increase in the electroactive area.

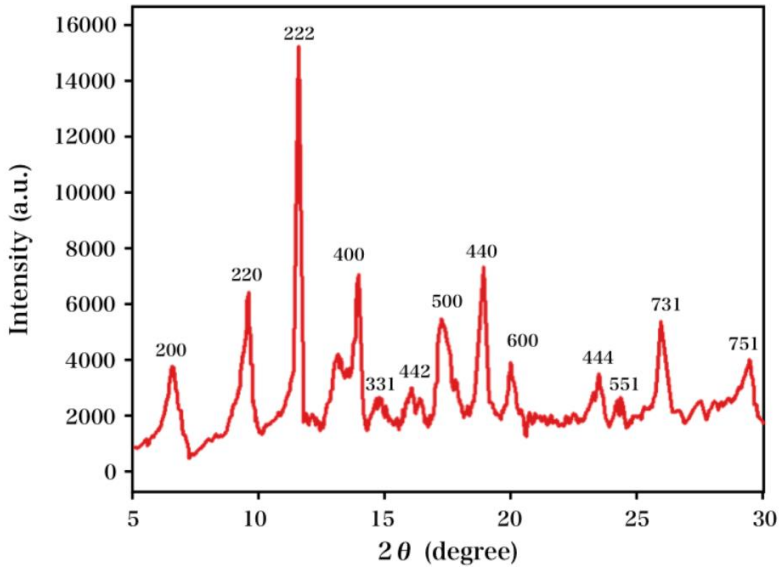

Figure 2. XRD profile recorded for the $[Cu(bpy)(H_2O)_2(BF_4)_2(bpy)]$ powder.

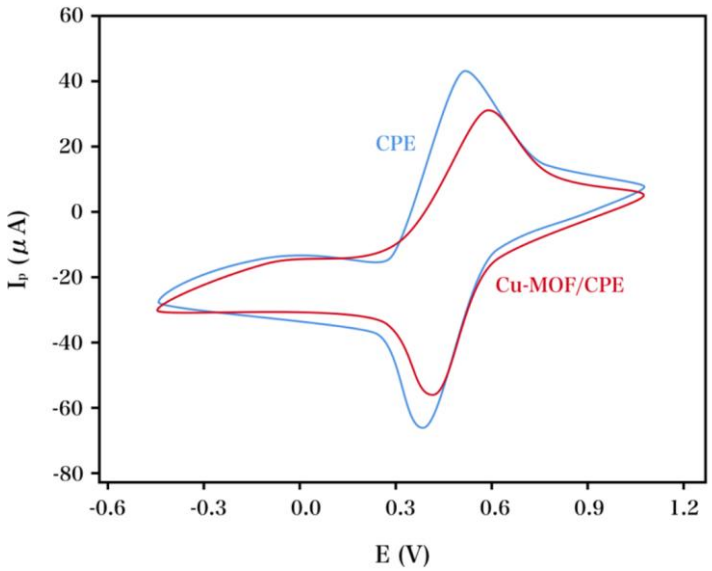

Figure 3. CVs recorded for the bare CPE and Cu-MOF/CPE in 60 μM $K_3[Fe(CN)_6]$. Scan rate: 100 mV/s, and pH: 7.2.

CV measurements were carried out to determine the electrochemical response at different concentrations of 2,4-DCP. The CVs of the oxidation of 2,4-DCP using varying electrodes in 0.2 M PBS at pH 7.2 (scan rate, 0.10 V/s; potential range, −0.4 to +1.0 V) are displayed in Figure 4. For both the bare and Cu-MOF-modified CPEs, broad single oxidation peaks were observed during scanning. For the bare CPE, an oxidation peak was observed in the presence of a specific concentration of 2,4-DCP (100 μM) at a potential of 0.67 V, and a peak current of 0.7 μA was obtained. For the CPE modified by the Cu-MOF, an oxidation peak was observed in the presence of a same concentration of

2,4-DCP (100 µM) at a potential of 0.71 V, and a peak current of 1.7 µA was obtained (2.3-fold higher than that of the bare CPE).

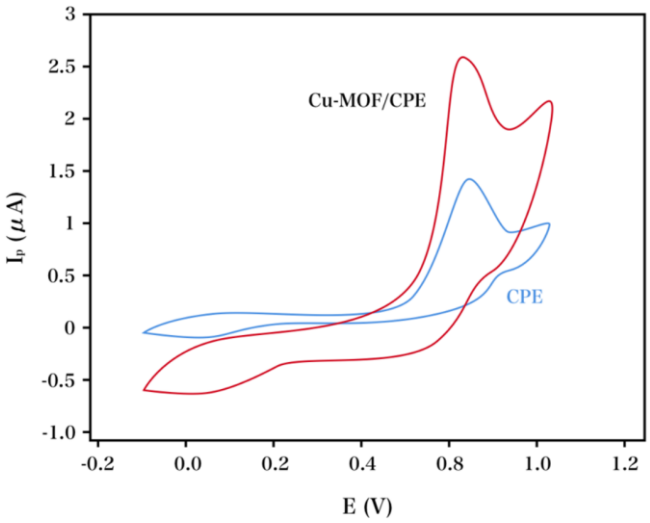

Figure 4. CVs recorded for the bare CPE and the Cu-MOF/CPE in 200 µM 2,4-DCP. Scan rate: 100 mV/s, pH: 7.2, and electrolyte: 0.1 M PBS.

The electrochemical analysis of 2,4-DCP was favorably realized using a highly sensitive and applicable amperometric strategy. Figure 5A and B shows the data and optimization of the test potential, respectively. Figure 5A displayed the hydrodynamic voltammogram (HV) of 2,4-DCP. With an increase in the applied potential, obvious increases in the anodic current response of 2,4-DCP and the background current were observed. Therefore, we studied the hydrodynamics of the signal-to-background ratio, not the current signal (Figure 5B). The signal-to-background ratio obtained at an applied potential of 0.74 V indicated the highest sensitivity for 2,4-DCP. Thus, the optimum amperometric potential was determined as 0.74 V and used for the following measurements.

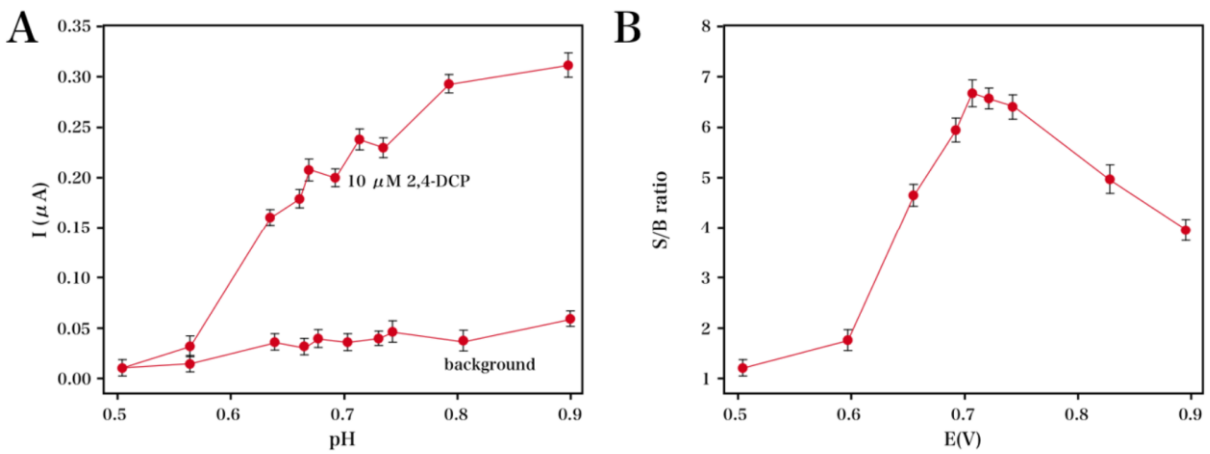

Figure 5. (A) Peak currents recorded for 10 µM 2,4-DCP and the background at the Cu-MOF/CPE; (B) Peak currents recorded for the signal-to-background ratios obtained from the results in (A). Scan rate: 100 mV/s, pH: 7.2, and electrolyte: 0.1 M PBS.

As shown in Figure 6, a linear relationship was found between the peak current (I_{pa}) and the concentrations of 2,4-DCP over a range of 4 to 100 μM under the optimal parameters, and the LOD was calculated as 1.1 μM.

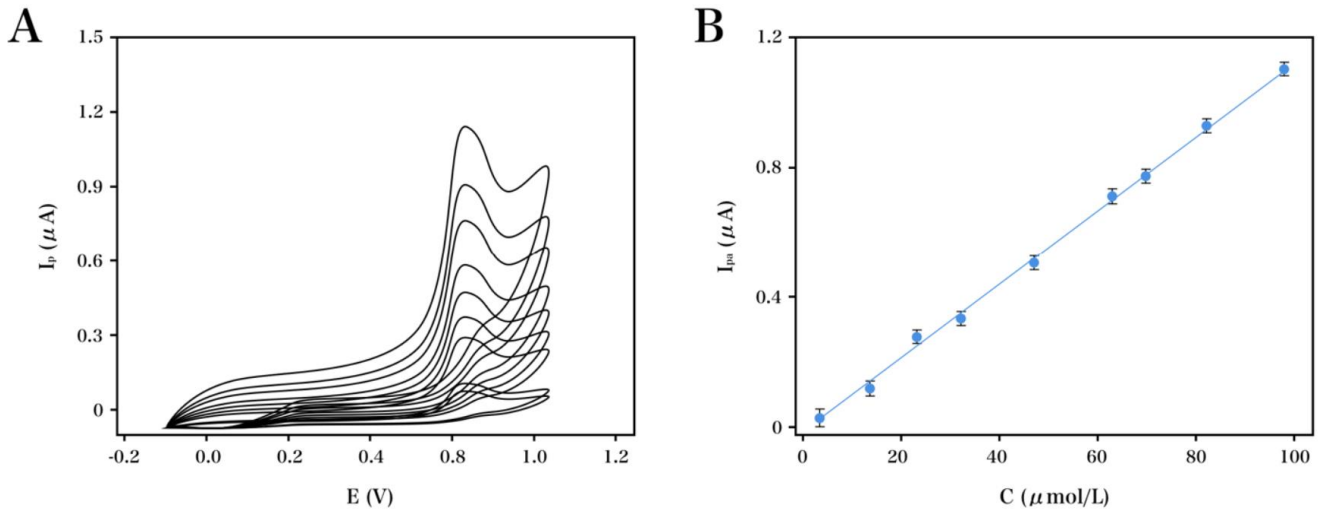

Figure 6. (A) CV curves and (B) calibration curve recorded for the amperometric response of varying concentrations of 2,4-DCP (10, 20, 30, 50, 70, 90 and 100 μM). Scan rate: 100 mV/s, pH: 7.2, and electrolyte: 0.1 M PBS.

The amperometric response of 2,4-DCP using the Cu-MOF/CPE was measured to study the electrode lifetime. Note that the electrode was stored in a refrigerator at 4 °C before use. After being continuously used for 15 days, the retained current response from the original value was obtained in a range of 97 to 108%, which suggested that our proposed sensor was highly stable for a long duration. For the inter-day and intra-day analysis of 2,4-DCP (100 μM), the relative standard deviations (RSDs) were obtained as 1.32% and 2.41% (n = 7), respectively. Therefore, our developed sensor was highly precise. The batch-to-batch reproducibility was studied using seven electrodes under optimal parameters; for the amperometric responses of the developed sensor, the RSD was calculated as 3.26%.

Table 1. Electrochemical detection of 2,4-DCP using our developed electrochemical sensor and those reported elsewhere.

Immunosensor	Detection range (μM)	Limit of detection (μM)	Reference
β-CDBIMOTs/CPE	4-100	1.2	[48]
Tyrosine/MWCNTs/GCE	2-100	0.66	[49]
MB-AG/GCE	12.5–208	2.06	[50]
HRP/MWNT/GCE	1.0–100	0.38	[51]
Cu-MOF/CPE	4–100	1.1 μM	This work

Our developed Cu-MOF/CPE exhibited a wider linear range, simpler electrode preparation, and a higher sensitivity than those reported elsewhere (Table 1). The results indicated the appropriateness of our proposed electrode for 2,4-DCP analysis. Additionally, its high sensitivity and low-cost fabrication pave the way for the development of new generations of green electrochemical sensors.

The application of the Cu-MOF/CPE for the detection of 2,4-DCP in environmental samples was studied by using two tap water samples and analyzing them according to the procedures used in the laboratory. Table 2 displays the concentration of 2,4-DCP in various environmental samples. The Cu-MOF/CPE` exhibited excellent performance for the detection of 2,4-DCP in four test environmental samples. Combined with a pretest evaluation, the Cu-MOF/CPE was found to be suitable as a compact electrochemical sensor for on-site environmental protection applications.

Table 2. The detection of 2,4-DCP in tap water specimens using the Cu-MOF/CPE.

Sample	Added (μM)	Found (μM)	Recovery (%)
Sample 1	0	0	—
	10	10.07	100.7
Sample 2	0	0	—
	15	14.95	99.67
Sample 1	0	0	—
	20	20.14	100.7
Sample 2	0	0	—
	30	30.50	101.67

4. CONCLUSIONS

The present study reported the simple synthesis of the MOF material $[Cu(bpy)(H_2O)_2(BF_4)_2(bpy)]$, and a highly sensitive and facile electrochemical sensor was developed based on the Cu-MOF/CPE for the analysis of 2,4-DCP. The results indicate that $[Cu(bpy)(H_2O)_2(BF_4)_2(bpy)]$ showed enzyme-like properties, strong adsorption capacity, and distinct charge transfer efficiency, which confirmed a remarkably increased oxidation peak current for 2,4-DCP.

References

1. X. Cui, W. Zuo, M. Tian, Z. Dong and J. Ma, *J. Mol. Catal A-Chem*, 423 (2016) 386.
2. W. Qin, M.E. Silvestre, G. Brenner-Weiss, Z. Wang, S. Schmitt, J. Hübner and M. Franzreb, *Sep. Purif. Technol.* 156 (2015) 249.
3. J. Sin, S. Lam, A. Mohamed and K. Lee, *Int. J. Photoenergy*, 2012 (2012) 88.
4. K. Henningsen and N. Boardman, *Plant. Physiol*, 51 (1973) 1117.
5. S. Dong, G. Suo, N. Li, Z. Chen, L. Peng, Y. Fu, Q. Yang and T. Huang, *Sensor. Actuat B-Chem*, 222 (2016) 972.
6. H. Shang, C. Yang and X. Yan, *J. Chromatogr. A*, 1357 (2014) 165.
7. M. Dincă, A. Dailly, Y. Liu, C.M. Brown, D. Neumann and J. Long, *J. Am. Chem. Soc*, 128 (2006) 16876.
8. M. Dincă and J. Long, *Angew. Chem. Int. Edit*, 47 (2008) 6766.
9. M. Allendorf, C. Bauer, R. Bhakta and R. Houk, *Chem. Soc. Rev*, 38 (2009) 1330.
10. W. Liu and X.B. Yin, *Trac-Trend. Anal. Chem*, 75 (2016) 86.
11. H. Park, J. Ulrich Mueller, J. Lee and J. Li, *Chem. Mater*, 19 (2015) 1308.

12. J.Liu, L. Pan, S. Simizu, B. Zande and J. Li, *J. Phys. Chem. C*, 112 (2015) 2911.
13. H. Wu, W. Zhou and T. Yildirim, *J. Phys. Chem. C*, 113 (2016) 3029.
14. T. Makal, A. Yakovenko and H. Zhou, *J. Phys. Chem. Lett*, 2 (2015)
15. B. Gui, X. Meng, H. Xu and C. Wang, *Chinese. J. Chem*, 34 (2016) 186.
16. H. Wu, B. Xia, L. Yu, X. Yu and X. Lou, *Nat. Commun*, 6 (2015) 6512.
17. H. He, Y. Song, F. Sun, Z. Bian, L. Gao and G. Zhu, *J. Mater. Chem. A*, 3 (2015) 16598.
18. H. Zubair and J. Hwa, *J. Hazard. Mater.*, 283 (2015) 329.
19. D. Saha and S. Deng, *J. Phys. Chem. Lett*, 1 (2016) 73.
20. M. Lalonde, O. Farha, K. Scheidt and J. Hupp, *Acs. Catalysis*, 2 (2015) 1550.
21. J. Tang, R.R. Salunkhe, J. Liu, N.L. Torad, M. Imura, S. Furukawa and Y. Yamauchi, *J. Am. Chem. Soc*, 137 (2015) 1572.
22. N. Campillo, P. Viñas, J. Cacho, R. Peñalver and M. Hernándezcórdoba, *J. Chromatogr. A*, 1217 (2010) 7323.
23. T. Ho, C. Chen, Z. Li, T. Yang and M. Lee, *Anal. Chim. Acta.*, 712 (2012) 72.
24. N. Fattahi, Y. Assadi, M. Hosseini and E. Jahromi, *J. Chromatogr. A*, 1157 (2007) 23.
25. S. Popov, Y. Chumichkina, E. Shapovalova, S. Dmitrienko and Y. Zolotov, *J. Anal. Chem*, 66 (2011) 6.
26. Y. Li, Y. Jiao, Y. Guo and Y. Yang, *Anal. Methods-UK*, 5 (2013) 5037.
27. Q. Liu, J. Shi, L. Zeng, T. Wang, Y. Cai and G. Jiang, *J. Chromatogr. A*, 1218 (2011) 197.
28. Q.Z. Feng, L.X. Zhao, W. Yan, F. Ji, Y.L. Wei and J.M. Lin, *Anal. Bioanal. Chem*, 391 (2008) 1073.
29. Q. Feng, H. Li, Z. Zhang and J. Lin, *The Analyst*, 136 (2011) 2156.
30. Q. Xu, X. Li, Y.E. Zhou, H. Wei, X.Y. Hu, Y. Wang and Z. Yang, *Anal. Methods-UK*, 4 (2012) 3429.
31. K. Omidfar, F. Khorsand and A. Darziani, *Biosens. Bioelectron*, 43 (2013) 336.
32. G. Mills and G. Fones, *Sensor. Rev*, 32 (2012) 17.
33. L. Xiao, R. Xu, Q. Yuan and F. Wang, *Talanta*, 167 (2017) 39.
34. Y. Song, C. Gong, D. Su, Y. Shen, Y. Song and L. Wang, *Anal. Methods-UK*, 8 (2016) 2290.
35. B. Rezaei, A. Ensafi and E. Jamshidi-Mofrad, *Sensor. Actuat B-Chem*, 211 (2015) 138.
36. L. Cui, J. Wu, J. Li and H. Ju, *Anal. Chem.*, 87 (2015) 10635.
37. L. Yang, C. Xu, W. Ye and W. Liu, *Sensor. Actuat B-Chem*, 215 (2015) 489.
38. J. Xu, J. Xia, F. Zhang and Z. Wang, *Electrochim. Acta*, 251 (2017)
39. J. Liu, H. Tang, B. Zhang, X. Deng, F. Zhao, P. Zuo, B.C. Ye and Y. Li, *Anal. Bioanal. Chem*, 408 (2016) 4287.
40. A. Wong, M. Foguel, S. Khan, F. Oliveira, C. Tarley and M. Sotomayor, *Electrochim. Acta*, 182 (2015) 122.
41. H. Hosseini, H. Ahmar, A. Dehghani, A. Bagheri, A. Tadjarodi and A. Fakhari, *Biosens. Bioelectron*, 42 (2013) 426.
42. Y. Fu, P. Li, L. Bu, T. Wang, Q. Xie, J. Chen and S. Yao, *Anal. Chem.*, 83 (2011) 6511.
43. D. Jiang, T. Mallat, F. Krumeich and A. Baiker, *J. Catal.*, 257 (2008) 390.
44. P. De Meester, D. Goodgame, A. Skapski and Z. Warnke, *Biochimica et Biophysica Acta (BBA)-Nucleic Acids and Protein Synthesis*, 324 (1973) 301.
45. N. Greenwood, *Chem. Soc. Rev*, (1959) 3811.
46. K. Lin, A. Adhikari, C. Ku, C. Chiang and H. Kuo, *Int. J. Hydrogen. Energ*, 37 (2012) 13865.
47. B. Panella, M. Hirscher, H. Pütter and U. Müller, *Adv. Funct. Mater*, 16 (2006) 520.
48. L. Kong, S. Huang, Z. Yue, B. Peng, M. Li and J. Zhang, *Microchim. Acta.*, 165 (2009) 203.
49. Y. Sun, L. Wang and H. Liu, *Anal. Methods-UK*, 4 (2012) 3358.
50. S. Huang, Y. Qu, R. Li, J. Shen and L. Zhu, *Microchim. Acta.*, 162 (2008) 261